

LattiSense: A 3D-Printable Resistive Deformation Sensor with Lattice Structures

Rei Sakura

The University of Tokyo
Tokyo, Japan
sakura@xlab.iii.u-tokyo.ac.jp

Keisuke Watanabe

The University of Tokyo
Tokyo, Japan
watanabe@xlab.iii.u-tokyo.ac.jp

Changyo Han

The University of Tokyo
Tokyo, Japan
hanc@nae-lab.org

Ryosuke Yamamura

R4D, Mercari Inc.
Tokyo, Japan
ryosuke-y@mercari.com

Yahui Lyu

The University of Tokyo
Tokyo, Japan
lyu@xlab.iii.u-tokyo.ac.jp

Yasuaki Kakehi

The University of Tokyo
Tokyo, Japan
kakehi@iii.u-tokyo.ac.jp

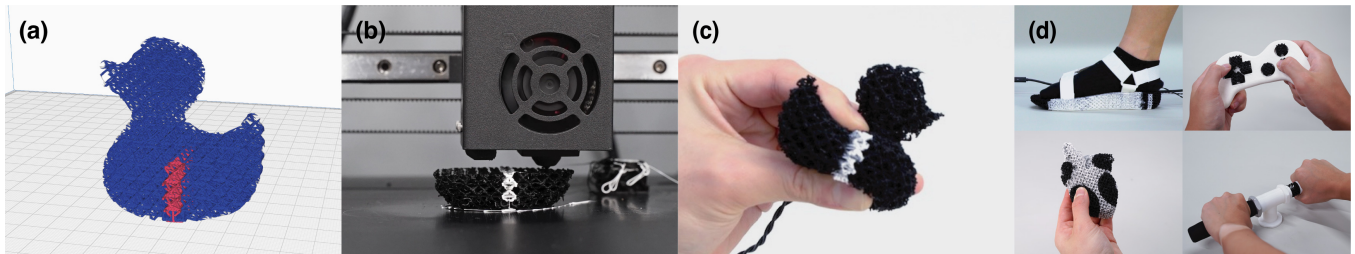


Figure 1: Overview of LattiSense. With LattiSense, (a) users can embed deformation-sensing capabilities into an existing 3D model. (b) After printing a 3D object with a dual-material 3D printer and post-processing, (c) the printed object can be instantly used as a deformable sensor. (d) LattiSense can be employed to fabricate various artifacts from wearable sensors to custom controllers.

ABSTRACT

Recently, soft and deformable materials have become popular as sensors for their applicability in daily objects. Although studies have been conducted on existing conductive soft materials, problems such as a lack of design freedom regarding softness, shape, and deformation, as well as wiring complexity remain. Here, we propose a novel soft sensor called LattiSense, fabricated using an FDM 3D printer. By arranging conductive and non-conductive flexible filaments in a lattice structure, we created a soft sensor designed with a high degree of freedom in terms of hardness, shape, deformation, and wiring paths. By modifying the lattice parameters, multiple modes of deformation can be designed. The softness can also be locally customized by adjusting lattice parameters. In this paper, we present the design and implementation of LattiSense and investigate its characteristics with respect to several parameters. We also demonstrate design software and several application scenarios.

CCS CONCEPTS

- Human-centered computing → Interaction devices.

KEYWORDS

3D printing; soft sensor; fabrication; deformable user interfaces

ACM Reference Format:

Rei Sakura, Changyo Han, Yahui Lyu, Keisuke Watanabe, Ryosuke Yamamura, and Yasuaki Kakehi. 2023. LattiSense: A 3D-Printable Resistive Deformation Sensor with Lattice Structures. In *Symposium on Computational Fabrication (SCF '23), October 8–10, 2023, New York City, NY, USA*. ACM, New York, NY, USA, 14 pages. <https://doi.org/10.1145/3623263.3623361>

1 INTRODUCTION

Soft materials have recently gained attention owing to their potential for natural interactions in our daily objects and interfaces [Boem and Troiano 2019]. In such objects, deformation of functional materials such as conductive foam [Nakamaru et al. 2017; Nguyen et al. 2015; Watanabe et al. 2021] may be used to detect user input.

However, such soft sensing techniques [Nakamaru et al. 2017; Nguyen et al. 2015; Parzer et al. 2017; Watanabe et al. 2021] have several limitations. First, their materials have uniform properties, making it difficult to design objects or structures with localized softness and sensitivity. Second, current soft sensing materials require manual processes or special fabrication equipment to make complex shapes, including three-dimensional (3D) shapes. Third, compression-based sensors [Aigner et al. 2022; Nakamaru et al.

Permission to make digital or hard copies of all or part of this work for personal or classroom use is granted without fee provided that copies are not made or distributed for profit or commercial advantage and that copies bear this notice and the full citation on the first page. Copyrights for components of this work owned by others than the author(s) must be honored. Abstracting with credit is permitted. To copy otherwise, or republish, to post on servers or to redistribute to lists, requires prior specific permission and/or a fee. Request permissions from permissions@acm.org.

SCF '23, October 8–10, 2023, New York City, NY, USA

© 2023 Copyright held by the owner/author(s). Publication rights licensed to ACM.

ACM ISBN 979-8-4007-0319-5/23/10...\$15.00

<https://doi.org/10.1145/3623263.3623361>

2017] are designed for a single mode of deformation i.e., deformation only in a set direction. To detect deformation such as shearing and torsion, several techniques are combined, thus complicating the design process.

In our work, we specifically focus on 3D printed [Gong et al. 2021; Schmitz et al. 2017] soft sensors. This is because 3D printing is a common technique employed to produce soft material objects [Schumacher et al. 2015; Sun et al. 2021a] through flexible materials or tuned internal structures. Ion et al. [Ion et al. 2016] have previously shown local softness or functional movements in a single print process. In addition, 3D printed sensors with flexible conductive materials have been proposed [Georgopoulou et al. 2021; Gong et al. 2021], but their shapes and deformations are limited to a planar ones. There is also the issue of low design flexibility in softness i.e. not being able to tune specific areas in softness. More practical issues such as wiring locations prevent wider use as well.

In this paper, we propose a novel soft sensor, called LattiSense, 3D printed through conductive flexible materials in a lattice structure degree of freedom of three-dimensional shapes and deformations by printing. By changing parameters such as size or model of the lattice structure, it is possible to fabricate 3D printed versatile soft sensors that can sense multiple deformations such as twisting, shearing, and compression. In addition, different local softness values can be obtained in a single print. The design of the internal conductive path allows for greater freedom in the selection of cable attachment points on printed objects, simplifying the sensor configuration and enhancing its aesthetics.

To facilitate easy fabrication of such soft sensors, we developed a software that enables users to embed deformation modes (twisting, shear, compression) and softness to the desired parts of a 3D model. This allows users to design soft sensors and objects that can detect multiple deformations with higher accuracy, even without specialized knowledge or experience.

The contributions of our research are summarized below:

- Integrated single-print fabrication technique for soft sensor that can detect multiple deformations (compression, twist, and shear)
- Evaluation of mechanical properties of fabricated materials i.e., relationship between the amount of deformation and the change in resistance for various lattice sizes and beam thicknesses.
- Design software that allows users to create products by selecting the mode of deformation, softness, and location to embed the soft sensor.
- Demonstration of applications that utilize multiple types of soft sensors.

2 RELATED WORK

2.1 Digital Fabrication of Soft Objects

In the field of digital fabrication, several methods have been proposed for creating objects with rigid bodies [Abdullah et al. 2021; Mueller et al. 2014; Zeng et al. 2021] as well as for creating 3D objects with soft bodies [Hudson 2014; Kumar et al. 2020; Pérez et al. 2015]. For example, methods for outputting soft felt-like objects using soft fibers have been developed [Hudson 2014], such as using a laser cutter to cut fabric and using thermal glue to stack

them as a 3D-shaped object [Peng et al. 2015]. *WraPr* [Leong et al. 2020] showed a spool-based method for creating soft 3D objects by wrapping thread onto a core.

In addition, by designing internal structures with softer materials, objects with locally different softnesses can be created [Bickel et al. 2010; Pérez et al. 2015; Schumacher et al. 2015]. While 3D printers that utilize photopolymerization technology can manufacture complex structures with soft materials, the Fused Deposition Modeling (FDM) technique faces challenges in printing such structures, leading to constraints in the fabrication method. While the mechanical properties of a specific structure (such as springs) are explored [He et al. 2019], it is challenging to apply the same knowledge to the entire structure of the printed object. Consequently, researchers are currently exploring the design of softness using structures that can be produced with the FDM method [Kumar et al. 2020; Sun et al. 2021b].

In our work, we create a soft sensor using the Fused Deposition Modeling (FDM), owing to its greater versatility. We create a lattice structure with tunable regions that allows us to design the softness of the sensor. A lattice structure was chosen as a structure that could be printed using FDM and designed parametrically.

2.2 Function Design using Internal Structures

Prior works have demonstrated functional properties by designing or tuning internal structures of 3D-printed objects. These include sound insulation by designing an internal structure that dampens sound vibrations [Cai et al. 2019; Matlack et al. 2016; Zhang et al. 2020], liquid flow control through capillary action [Dudukovic et al. 2021] or tether-based shape constraints for printed inflatables [Han et al. 2021]. Some integrated rotary encoders into fabricated objects to sense mechanical movements [Alalawi et al. 2023]. In addition, change of internal structures has also been used for object identification [Dogan et al. 2020; Kubo et al. 2020; Yamamoto et al. 2021].

Gases are compatible with soft sensors because they do not affect the softness or deformation of flexible materials. Soft sensors that detect deformations from changes in air pressure [He et al. 2017; Truby et al. 2022] use internal flow path of a flexible material to detect pressure changes. However, sensors that use air pressure require large external devices such as air compressors, and wiring becomes complex when data needs to be collected for each flow path.

Recently, metamaterial mechanisms compatible with FDM 3D printing have been shown in the field of HCI [Han et al. 2021; Ion et al. 2018]. Similar approaches include assembled modularized units [Jenett et al. 2020] for stiffness, and reconfigurable metamaterials [Yang et al. 2022] for elasticity by activating or deactivating springs. Of particular interest to our work is the relationship between internal structure and object deformation [Abueidda et al. 2017; Coulais et al. 2016; Hazrat Ali et al. 2021; Sun et al. 2021a,c]. We drew inspiration from prior work in 3D-printed objects, where lattice structures are used for various mechanical deformation modes such as compression, twisting, and shearing [Wang and Liu 2020; Zhong et al. 2019].

In our work, we have applied conductive flexible materials to a technology that allows softness and deformation to be designed by the internal structure. This allows for different deformations

with structures and allows for the fabrication of a soft sensor with simple sensing configurations.

2.3 Deformable Sensors Using Conductive Materials

In soft interfaces composed of non-rigid materials, inputs with deformable sensors have been attracting attention [Boem and Troiano 2019]. Deformable sensors detect different types of deformations depending on the material and design method. *Flexibles* [Schmitz et al. 2017] are 3D-printed capacitive deformable sensors with internal conductive parts. This is a sensor that utilizes existing touch devices such as tablets, and these rigid devices reduce scalability and versatility.

Deformable sensors made entirely of soft conductive material such as conductive foam [Nakamaru et al. 2017; Nguyen et al. 2015; Watanabe et al. 2021], elastomer [Yoon et al. 2017, 2018], and yarn [Luo et al. 2021; Parzer et al. 2017; Schwarz et al. 2010; Shahmiri et al. 2019; Wu et al. 2020]. However, sensors using these existing materials have the problem that it is difficult to design shapea and softness due to the uniform properties of the materials.

To add deformation-sensing capabilities to internal structures using conductive materials, Helou et al. proposed a logic-circuit-type soft sensor that responds to deformation by designing switchable conductive pathways in the internal structure[El Helou et al. 2021]. In *Metasense* [Gong et al. 2021], capacitive compression and shearing are sensed through conductive filaments made of copper and non-conductive flexible filaments in the internal structure. However, these sensors still have issues such as wiring complexity and difficulty in creating custom 3D shapes.

Researchers have tailored sensor design as per deformation modes to be detected individually. Slyper et al. proposed a switching-type deformable sensor that uses elastomers and copper electrodes [Slyper et al. 2010]. To distinguish different deformation modes, such as twisting or bending, the shape and location of the electrodes need to be designed. *FoamSense* [Nakamaru et al. 2017] is a resistive deformable sensor based on a porous material coated with conductive ink. It is possible to change the deformation mode to be detected by altering the conductive part design and location of the electrodes. This offers deformation modes such as compression, twisting, bending, and shearing.

In our work, a soft sensor is created by 3D printing conductive flexible material in a lattice structure that can sense multiple deformation modes, including compression, twist, and shear. By varying the lattice structure patterns corresponding to the sensor location, we design various structures that deform as expected. Within a single-print 3D structure, we detect deformation quantities in various modes for sensing.

3 LATTISENSE

3.1 Overview and Design Properties

We propose a 3D soft sensor, LattiSense, constructed as a single piece using a commonly sold FDM-type 3D printer. Users can easily deform the fabricated sensor by using their fingers or palms.

To enable this deformation, LattiSense utilizes a 3D lattice structure (Fig. 2). A lattice structure is a type of cellular structure in which the unit structure is periodically arrayed. Lattice structures, which

are difficult to be manufactured by subtractive manufacturing, are commonly regarded as Design for Additive Manufacturing (DfAM) because they are easier to create owing to the manufacturing process of 3D printing [Yunlong Tang 2016]. Lattice structures are generally characterized by their lightweight, but using flexible materials also makes them suitable for creating soft three-dimensional objects [Wu et al. 2021]. In flexible lattice structures, it is possible to control the deformation and softness by changing parameters such as the model and size of the unit lattice.

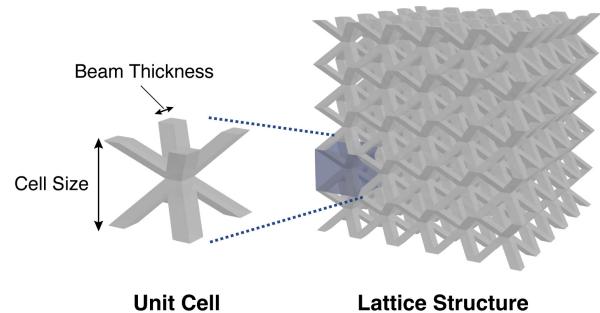


Figure 2: Three-dimensional lattice structure and its parameters.

A novel aspect of this study is the use of this structure for deformation sensing. By utilizing a parametrically designable lattice structure, it is possible to design properties such as softness that are difficult to adjust with conventional soft sensors. To detect deformation, a lattice structure was constructed using conductive flexible filaments. When this structure is deformed, the resistance in the deformed area changes. LattiSense can be used as a sensor by reading the change in resistance in real time.

The wires were attached to the sensor to externally measure the resistance. To obtain the resistance value, at least two wires must be attached so that the measured area is sandwiched between them. As mentioned in *FoamSense* [Nakamaru et al. 2017], which also uses resistance changes detected in porous materials for deformation acquisition, wires are attached to the bilateral surfaces of the object, namely the top and bottom surfaces, according to the direction of the deformation. However, these wires may make contact with the fingers in some positions, which may interfere with the deformation interactions. Therefore, we developed a design that increased the flexibility of wire placement for LattiSense. Specifically, a part of an object was replaced with a non-conductive filament, and the shortest conductive path between the wires was designed. This enhances the freedom to select wire attachment points, such as by taking two wires at almost the same point on the same surface.

Based on the above basic principles, the properties that can be designed in LattiSense are summarized below (Fig. 3).

Shape Flexibility in designing any 3D shape allowed by a FDM printer, wherein the entire object or a specific region of the object may be used as a sensor.

- Deformation mode** Mode Control of amount of deformation under compression, shear and/or twisting forces, where such control is fabricated tuned unit lattice structure.
- Softness** Softness can be altered by changing the cell size of the lattice structure and the beam thickness. It is also possible to locally design different softness values.
- Wiring arrangement** Arrangement Wires can be placed at the desired position without interfering with interactions or other parts during deformation.

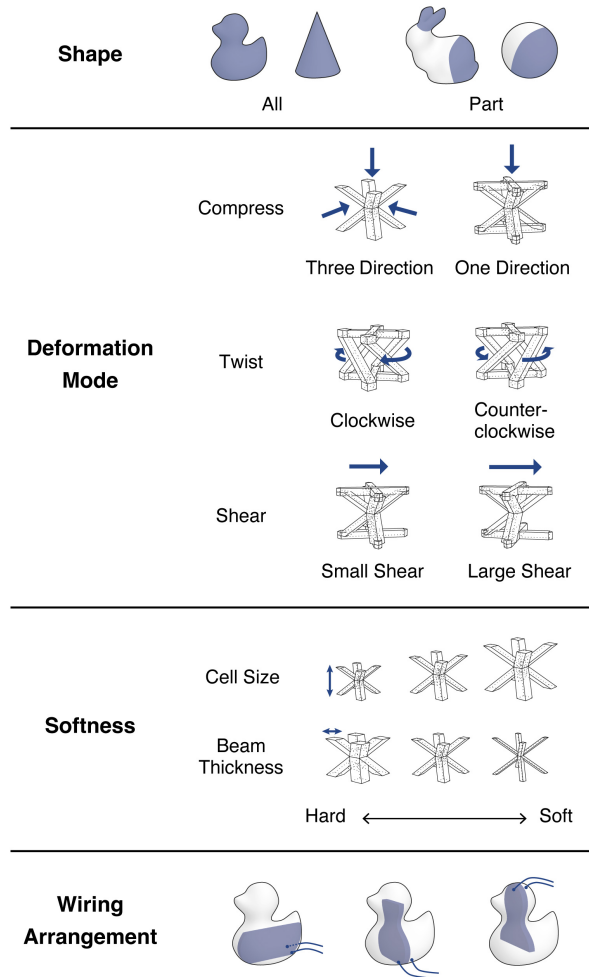


Figure 3: Design properties of LattiSense.

The design details of each property are described below.

3.2 Shape Design

LattiSense can be created in any 3D shape. By embedding a lattice structure into an entire object or a specific part of the object, it can be used as a sensor. Because it is difficult to print parts that hang in mid-air in FDM 3D printing, such as bridges, in LattiSense, the lattices are arrayed along the curved surface of the object to ensure

that the beams of the structure do not float in the air. This arrangement method enables the stable printing of curved 3D shapes, even with the FDM technology. Details of this algorithm are described in the Fabrication section.

3.3 Deformation Mode

Different types of deformations are possible depending on the unit lattice structure. In LattiSense, the deformation of compression and the accompanying twisting and shearing deformations can be realized. Each deformation is shown in Fig. 4, and their corresponding unit 3D model is shown in Fig. 3. In the following, the xy-plane when a force is applied from the z-axis direction is referred to as the “compression plane,” and deformation directions are described based on this plane. Regarding the names of the structural parts, the edges parallel to this plane are referred to as frames, whereas the other parts are described as beams (Fig. 5).

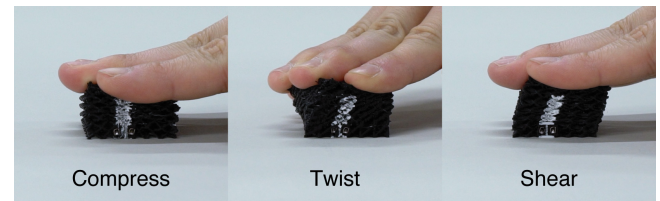


Figure 4: Deformation of 3D printed objects.

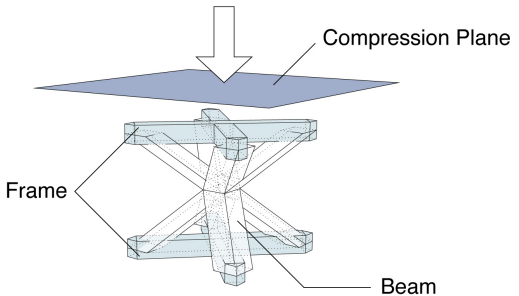


Figure 5: Definition of terms of the structural parts of a unit lattice structure.

Detailed explanations of each deformation structure follow.

3.3.1 Compress. One possible structure that can be pushed into is a lattice structure based on a body-centered cubic structure. In LattiSense, an edgeless body-centered cubic structure is adopted as the compression structure for softness. This structure is isotropic and can be pushed in all three directions, perpendicular to the surface. If the deformation direction is defined as a single direction, the frame can be attached to a plane that is parallel to the compression plane. The possible frames are those that connect diagonals (cross frame) and those that connect edges (edge frame). In the latter frame, as shown in the previous experimental results from Sakura

et al. [Sakura et al. 2022], the deformation is stepwise; hence, the cross frame is used to specify the direction.

3.3.2 Twist. Referring to the studies conducted by Wu et al. [Wu et al. 2021] and Zhong et al. [Zhong et al. 2019], we created a structure based on a face-centered cubic structure with one diagonal line on a face perpendicular to the compression plane. The inclination of this diagonal determines the rotation direction of the twist. For frames, there are two possible patterns: one connecting the edges and the other connecting the diagonals. For surfaces parallel to the compression plane, we used a cross frame, which was also considered in the study conducted by Wu et al. [Wu et al. 2021]. As pointed out by Zhong et al. [Zhong et al. 2019], this structure has a problem in that the rotation is restricted by the adjacent unit lattices in the direction horizontal to the compression plane. To solve this problem, the unit structures were arranged sequentially, thereby reducing some of the constraints.

3.3.3 Shear. A shear structure was created by removing the lowest of the eight beams from the compression structure. When force is applied from the above, shearing occurs in the direction of the missing beam. Without the frame, the push-in force is dispersed, resulting in a small amount of shearing; therefore, we installed a cross frame in the same manner as used for twisting. Removing the two beams increases the shear but also increases the difficulty of printing; therefore, it is not suitable for creating large sensors.

3.4 Softness

The softness of an object can be adjusted by changing its lattice parameters. The parameters are the cell size and the beam thickness. The larger the cell size and the thinner the beam thickness are, the softer the object. Because LattiSense can embed different structures in separate parts of an object, it is also possible to locally change its softness.

3.5 Wiring Arrangement

LattiSense can place two wiring points together in close proximity by partitioning conductive cells by non-conductive cells. This partition, composed of non-conductive filaments, is referred to as separator in this study. The structure of the separator is illustrated in Fig. 6. As wires can be grouped together, users can take wires from any desired part of the object and keep them out of the way of deformation. The user determines the wiring points, and positions the separator so that it crosses the two wiring points and is perpendicular to the compression plane. This results in a structure in which the conductive part that detects deformation is folded back, allowing the wiring at the desired wiring points to detect the resistance change caused by compression. The connector parts should be placed at the wiring points so the contact pins can be thermally press-fitted. The connector parts are described in detail in the Fabrication section.

3.6 Calibration

Deformation of LattiSense is detected by reading the resistance change. In the calibration phase, the resistance is measured at the standard state and the completely deformed state. Those two values are considered upper and lower limits. The resistance change of

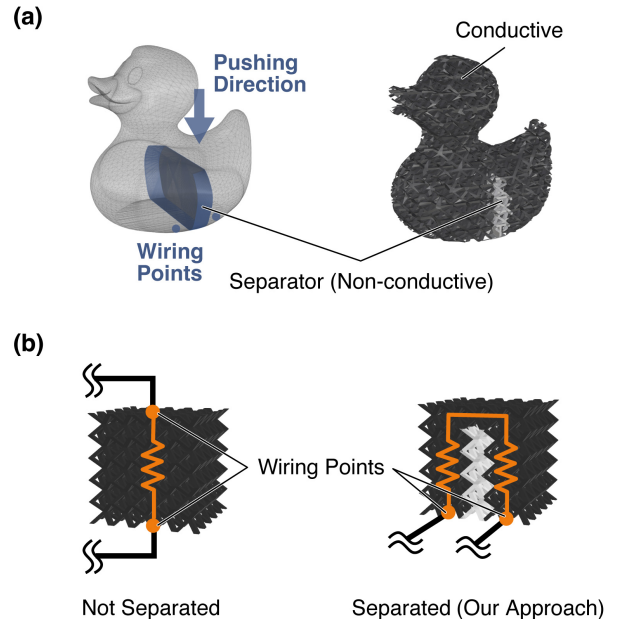


Figure 6: (a) Separation Structure. (b) Comparison of wiring with/without separator.

LattiSense is close to linear behavior (Fig. 14); the deformation can be estimated from the resistance. Repeated deformation may change the initial resistance, so it is desirable to perform calibration in such cases. Based on the experimental results of Sec. 5.3 Durability, we assume that calibration is recommended after 1,000 cycles of deformations.

4 FABRICATION

LattiSense is created by first generating 3D model data of the sensor, 3D printing it, and attaching the connector parts. Each of these steps is described in detail below.

4.1 Design Software

We developed design software to support the design and modeling of LattiSense. This software was developed using the 3D CAD software, Rhinoceros, and its Grasshopper plugin. The user interface is executed using this software. Using this software, users can generate 3D model data of the sensor. Fig. 7 shows the interface screen of the software and the operation procedure. The details of the procedure are as follows.

- (1) Import the 3D model data to embed the sensor.
- (2) Select the area where the sensor is to be embedded.
- (3) Select the deformation mode.
- (4) Determine the softness.
- (5) Select the wiring point.
- (6) Export the STL files.
- (7) The same procedure as that reported in (2)–(6) is applied to for the other embedding areas.

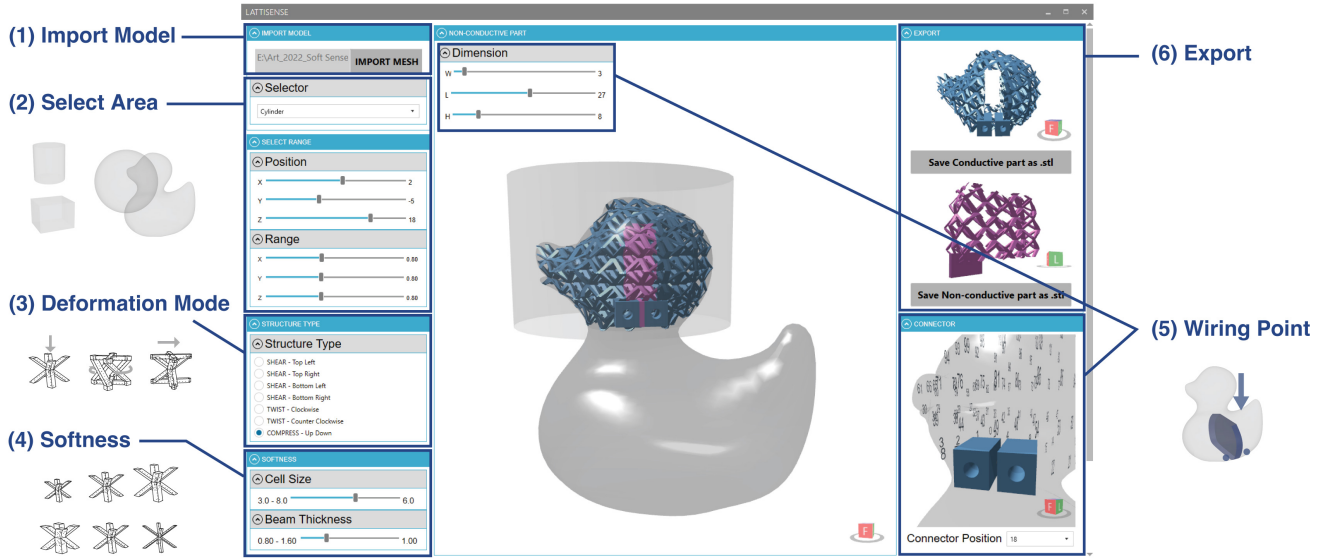


Figure 7: Design software and its operation procedure for LattiSense.

Import Model and Select Area. First, the user imports a 3D model and selects the area to embed the sensor. To select this area, in addition to the basic shapes of the cylinders, spheres, and rectangles, any imported shape can be used as a selector. The size and position of the selector can be adjusted using sliders, and the area that overlaps the object can be selected as the embedded area.

Select Deformation Mode. Deformation modes can be selected from the three modes described above: compression, twisting, and shearing.

Determine Softness. Softness can be changed by adjusting the cell size and beam thickness. When users move the slider, the cell size or beam thickness changes accordingly, and the 3D model in the preview also changes responsively. As mentioned above, the larger the cell size and the thinner the beam, the softer the sensor. The slider range for cell size is from 3.0 mm to 8.0 mm, and that for beam thickness is from 0.8 mm to 1.6 mm. This value is roughly defined based on experimental results, but it is not designed to guarantee printability. This is discussed in detail in the Discussion section.

The software generates a unit lattice structure based on the selected deformation mode and softness. The unit lattice structure is arrayed within the 3D region. The algorithm is illustrated in Fig. 8. First, (1) the 3D shape mesh data is divided into (2) voxels according to cell size. Then, (3) the vertices of the voxels outside the mesh are moved to the closest points on the mesh such that they are aligned with the mesh surface. Lastly, (4) the structures of the selected deformation modes are morphed and placed on the voxels created to fit the 3D model. The "Morph To Twisted Box" component of Pufferfish¹, a Grasshopper plug-in, was used for this morphing. The structure is deformed and placed such that each

vertex of the basic unit lattice fits the vertex of the voxel to be placed.

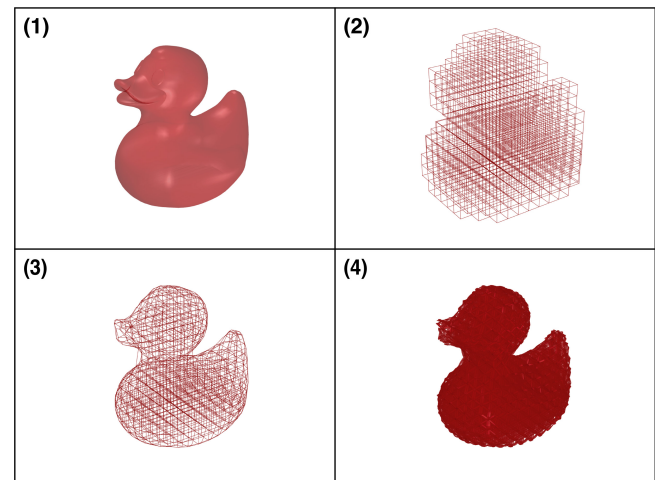


Figure 8: Algorithm for arranging lattice structures on a 3D surface: (1) A mesh data is (2) divided into voxels. (3) The vertices outside the mesh are moved to nearby mesh surface. (4) The structures are morphed and placed on the voxels.

Wiring Points. The wiring points can be selected from cells on the outer side. The cells are numbered; therefore, the number can be selected from the drop-down list. The connector parts are placed at the position of the selected cell, and a separator is created according to this position. The size of the separator can be adjusted by using a slider.

¹<https://www.food4rhino.com/en/app/pufferfish>

Export. Finally, users obtain two data types as STL files: parts to be printed using conductive filaments and parts to be printed using non-conductive filaments.

4.2 3D Printing and Thermal Press-Fitting

After creating the 3D model data, the next step is 3D printing and post-processing. The procedure is as follows:

- (1) Slice the 3D model.
- (2) Perform 3D printing.
- (3) Thermal press-fit contact pins.

Ultimaker Cura was used as the slicer, and the TENLOG TL-D3 Pro was used as the dual-head FDM printer for 3D printing. NinjaTek's Eel filament was used as the conductive TPU filament, and 3DXFLEX's flexible TPU filament was used as the non-conductive TPU filament. Both filaments have a Shore hardness of 90A; thus, the non-conductive and conductive sections would be equally soft when they have the same internal structure. Both filaments had diameters of 1.75 mm. The nozzle diameter was 0.4 mm and the nozzle temperature was 225°C for both conductive and non-conductive filaments. The printing speed, layer height, and infill were 15 mm/s, 0.2 mm, and 100 %, respectively.

As for the cross frame, when sliced as it is, the G-code path does not cross the diagonal line and turns at the center point (Fig. 9 (a)). Along this path, the center point hangs in the air, resulting in low print quality. Therefore, we created the frame part separately for each layer in the 3D model data, so that a general slicer could generate a crossing toolpath. This time, as the layer height was 0.2 mm, we generated a path that draws a diagonal line across the center point by dividing it into 0.2mm of layers each, as shown in Fig. 9 (b).

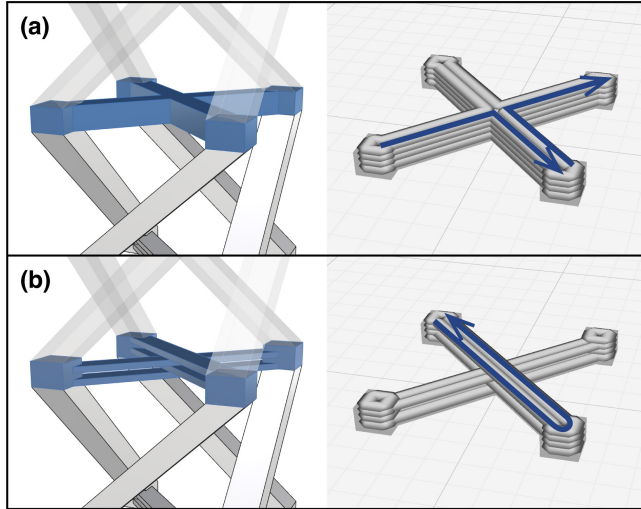


Figure 9: 3D model data and G-code generated by slicer: (a) For the model not divided into layers, the toolpath turns at the center of the crossing section, resulting in low print quality; (b) for the model divided into layers, the path is a diagonal line across the center point, resulting in high print quality.

Contact pins were thermally press-fitted into the holes of the connector parts using a soldering iron. The metal and conductive printed material were firmly bonded via thermal press-fitting to ensure the conduction between them. The connector parts are shown in Fig. 10.

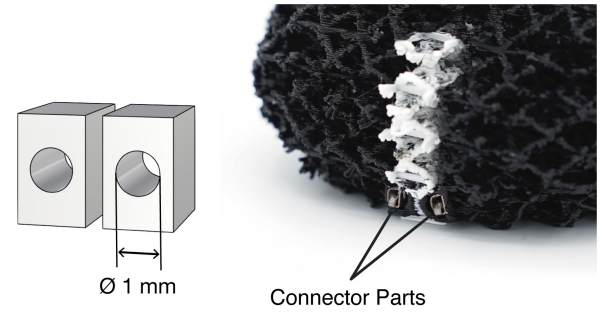


Figure 10: 3D model of the connector parts and contact pins thermo-press-fitted into connector parts

Examples of the output produced by the above procedure are shown in Fig.1 (c) and (d).

5 EVALUATION

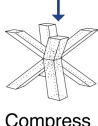
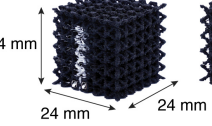
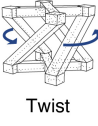
Unit Cell Structure	Cell Size		
	4.0 mm	4.8 mm	6.0 mm
			
			
			

Figure 11: Printed deformation structure samples (compression, twist, and shear) for compression test. Beam thickness was fixed at 0.8 mm. Unit cell size was 4.0, 4.8, and 6.0 mm.

We conducted experiments to investigate the relationships between the resistance and mechanical properties of objects printed under various parameters, expecting that they help users select appropriate lattice parameters. Cubic samples with 24 mm sides

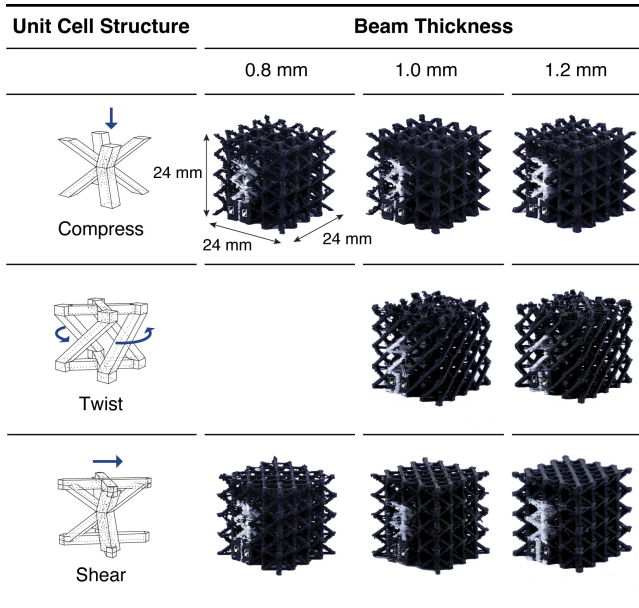


Figure 12: Printed deformation structure samples (compression) for compression test. Unit cell size was fixed at 6.0 mm. Beam thickness was 0.8, 1.0, and 1.2 mm.

were used in all experiments. The printed samples are shown in Figs. 11 and 12.

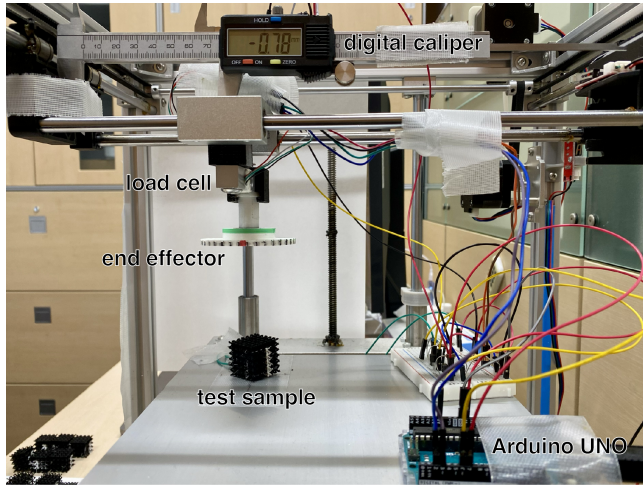


Figure 13: Photograph of the measurement equipment. The load cell is attached to the 3D printer carriage to measure the force against compression.

5.1 Test Apparatus and Measurement Procedure

The 3D printer was modified as the test apparatus, as shown in Fig. 13. We installed a micro-beam-type load cell (SC133) and load cell controller (HX711) in the carriage and calibrated them using a weight scale. The stepper motors of the 3D printer were turned

off, except for those in the z-axis, to enable the carriage to move along the xy-plane. The x-axis belt of the 3D printer was removed to reduce friction along the x-axis. A digital caliper was attached parallel to the x-axis to measure translation along the x-axis. At the load point of the load cell, we attached a 3D-printed end effector with an internal ball bearing such that it could be rotated around the z-axis to measure the rotation angle of the test samples. The rotating end effector had a disk shape with a diameter of 60 mm. A web camera (Logitech BRIO) was used to capture the entire setup image.

The test samples were placed below the end effector and slowly compressed by raising the bed while the force and resistance values of the samples were measured using a microcontroller (Arduino UNO). The resistance values were measured using a voltage divider circuit and the internal AD converter of an Arduino UNO. The resistance of the resistor connected in series to the sensor was 2 k Ω . For the shear experiment, the translation along the X-axis was recorded by reading digital caliper digits using an Arduino UNO. For the twist experiment, we marked the upper side of the end effector in green for reference and marked the rotating part with a red dot. We calculated the angle of rotation by color tracking using OpenCV; however, the torque was not recorded. Each sample was compressed and released ten times (10 mm each).

5.2 Measurement Results

First, we investigated the relationship between the lattice size, beam thickness, and softness. The softness of the sensor can be controlled by changing the parameters of the lattice structure. The design tool allows the softness to be adjusted by changing the unit cell size and beam thickness, and the relationship between the softness and such parameters was investigated by measuring the force-displacement curve. The side length of the cubic samples were 24 mm. We compared the unit cells of three sizes: 4.0, 4.8, and 6.0 mm, which corresponded to the lengths of one side of the test samples divided by six, five, and four, respectively as shown in Fig. 11. We printed variations with sizes of 0.8, 1.0, and 1.2 mm to verify the effect of beam thickness. Three samples were printed for each design to investigate the variance between the samples. The twist deformation model with a 6.0-mm unit cell size and 0.8-mm beam thickness was excluded because the printed object was easily broken.

The relationship between the lattice size, beam thickness, and softness for the compression deformation models is shown in Fig. 14 (a). The dots indicate the measured data points, and the solid lines represent the mean values calculated from the data points for each sample. The fills on the lines represent distributions with 2σ . The arrows indicate the direction of press and release.

The results reveal that the larger the size of the unit cell, the softer it becomes, indicating that softness can be designed by adjusting the unit cell size. The structure becomes stiffer as the beam thickness increases. The overall softness of the printed sensors can be designed by combining these two parameters.

The resistance decreases when the sensor is pressed. This is presumably due to the increased density of the sensor. This indicates that the resistance values can be used to estimate the amount of deformation; therefore, the printed structure can function as a

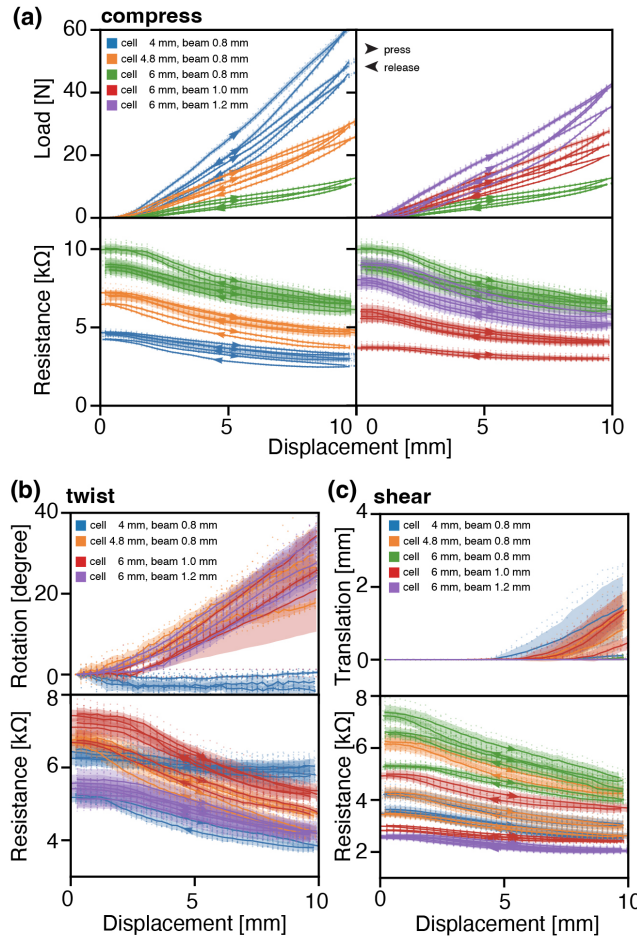


Figure 14: Mechanical properties of the printed deformation structures. (a) Force-displacement and resistance characteristics of the compress model with different unit cell size and beam thickness, (b) rotation characteristic of the twist model, and (c) lateral translation of the shear model.

deformation sensor. The resistance of the sensor was lower when the unit cell size was smaller. For beam thicknesses, the sample with a 1.0-mm beam thickness showed the lowest values. This is contrary to our assumption that, as the beam thickness increases, the resistance decreases owing to the increased density. Possible factors are that the gap is larger when the beam is thicker, depending on the relationship between the beam thickness and the extrusion width, or that there is a difference in the printing path depending on the beam thickness.

Given that each printed sensor exhibits variation in resistance values, these ranges can be calibrated to estimate the degree of deformation. Assuming a linear relationship between displacement and resistance values, linear regression can be employed for each calibration cycle. For instance, consider the third compress sample with a unit cell size of 6 mm and a beam thickness of 0.8 mm. The regression coefficients for resistance versus displacement were as

Table 1: Young's modulus of each unit cell size and deformation structure. Beam thickness was maintained at 0.8 mm. Units are N/m^2 (Pa).

unit cell size	compress	twist	shear
4 mm	2.03×10^5	1.61×10^5	2.28×10^5
4.8 mm	1.21×10^5	0.79×10^5	1.60×10^5
6 mm	0.51×10^5	<i>N/A</i>	0.73×10^4

Table 2: Young's modulus of each beam thickness for the compress deformation structure. Unit cell sizes are fixed at 6.0 mm. Units are N/m^2 (Pa).

beam thickness	compress	twist	shear
0.8 mm	0.51×10^5	<i>N/A</i>	0.73×10^5
1.0 mm	1.04×10^5	0.51×10^5	1.46×10^5
1.2 mm	1.56×10^5	0.61×10^5	2.48×10^5

follows: coefficient: -2.33, constant: 24.0, and coefficient of determination (R^2): 0.92. Across all samples, the R^2 values ranged from a minimum of 0.71 to a maximum of 0.93. This suggests that deformation can be approximately predicted from the measured resistance values.

Figure 14 (b) shows the amount of rotation when the twist deformation model is pressed. No obvious rotation was observed at a unit cell size of 4.0 mm, but at 4.8 mm and 6.0 mm, a rotation of approximately 30 degrees was observed regardless of the beam thickness. This rotation is noticeable when pressed by a human hand.

Figure 14 (c) shows the amount of shear (translation in the lateral direction) when the shear deformation model was pressed. The shear was obvious at specific combinations of parameters: 4.8 mm cell size and 0.8 mm beam thickness, 6.0 mm cell size and 1.0 mm beam thickness. This result indicates that an appropriate stiffness is required to make the structure apply lateral force.

The range of resistance change basically follows the density of the structure; however, there is considerable variance between samples. This variance can be resolved by applying the calibration process per each sensing structure.

The measured force-displacement curve was converted to a stress-strain curve to calculate the stiffness (Young's modulus) of the deformed structures. The calculated Young's moduli are listed in Tables 1 and 2. For every deformation model, the structure softened as the unit cell size increased. It is also observed that a smaller beam thickness resulted in a softer structure. The resulting Young's modulus was several hundred kPa , which is comparable to those of PDMS (about 360 kPa) and silicone elastomers (Ecoflex 00-10: 50 kPa).

5.3 Durability

To confirm the repeated usage behavior of the sensors, we measured the stiffness and resistance characteristics of a particular sample. We selected a sample with a 6.0-mm unit cell size and 0.8-mm beam thickness. This sample was assumed to have the least durability stemming from its thin beams or other manufacturing defects. Using

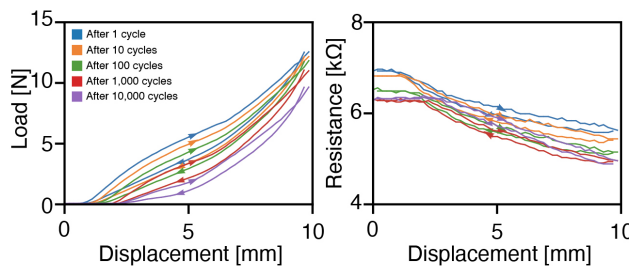


Figure 15: Result of the durability test. The test sample had unit cell size of 6.0 mm and beam thickness of 0.8 mm.

the apparatus shown in Fig. 13, we repeatedly pressed and released the sample by 10 mm 10,000 times.

The results are shown in Fig. 15. The lines represent the sensor characteristics after a certain number of measurement cycles. After 10,000 cycles of deformation, the sample maintained its shape and did not fall apart; however, the height of the sensor permanently decreased by approximately 2 mm. Owing to the decrease in height, the force-displacement curve shifted slightly to the right, but the steepness (softness) did not change significantly. The initial resistance value also decreased by less than 1 $k\Omega$, and the starting point of value change shifted to the right. These slight shifts can be calibrated appropriately after many cycles of deformation. The results suggest that despite permanent deformation, the 3D printed lattice sensor will still function as a sensor after many deformation cycles.

6 APPLICATIONS

We prototyped four possible application scenarios using LattiSense.

6.1 Shoe Sole Sensor

The first application of LattiSense is in the fabrication of a wearable sensor. Because its shape, stiffness, and sensing area can be designed with a certain degree of freedom, we believe that LattiSense is suitable for application in sensor devices used close to the human body.

We prototyped a shoe sole (Fig. 16) that could measure changes in force application using LattiSense. In this prototype, we used open-source sandal data reported on Fabbler² to embed the sensors. The sole was 10.3 cm wide, 25.0 cm long, and 3.6 cm thick, and could be worn. The sensors were embedded in two areas, the toe and heel, and they can sense the degree of deformation in each area. The accumulated data can be utilized for tracking user movements or estimating posture. This time, tilted left and right push-in cannot be identified, but if identification is required, sensors can be separately embedded on the left and right sides. The overall softness does not change with more sensors, but the number of wires increases.

Figure 16 (b) shows an example of the sensor output when a foot is placed on the sensor and a force is applied.

²<https://fabbler.cc/mippu/xcloudsandals>

6.2 Game Controller

Next, we leveraged the LattiSense features to create a game controller prototype with compression, as well as twist and shear buttons that can be 3D printed into a single piece as shown in Fig. 17.

Although there are many game controllers in the market, they have predetermined sizes and shapes. Therefore, children or people with disabilities may have problems with them as they do not fit their hand sizes or are too heavy to play with. Our prototype controller is 13.5 cm wide, 8.4 cm high, and 2.6 cm deep, with buttons in easy-to-press positions. This size and button hardness can be customized for user comfort.

In addition, in a typical controller, all buttons provide the same haptic design even though they have different functions. Our controller provides a passive haptic experience that corresponds to this function. For example, as they are pressed, the up button shears upward, and the rotate button rotates by approximately 20 degrees. This is thought to lead to a more intuitive user experience.

6.3 Educational Instrument (Interactive Heart Model)

The third application was an interactive physical model for educational purposes. In actual educational settings, such as models that consider topographic features and living creatures, instruments are often used to learn about a model's shape, structure, and size by touching it. There is also a need for 3D printers to create three-dimensional educational materials.

We created a soft prototype of an educational model that allows interaction through deformation by leveraging the features of LattiSense (Fig. 18). The prototype is based on the shape of the heart (the original data were from thingiverse³). In the first application, when a part is pressed, it will illuminate the illustration on the screen to show its name. The user can memorize the part by checking the shape of the heart in their hands (Fig. 18 (a)). The second application was cardiac massage training. Cardiac massage should be performed with a consistent rhythm and force, but there are few tools to easily obtain feedback on rhythm and force (Fig. 18 (b)). When this model is deformed by pressing from above, the number of presses and their rhythm will be shown on the screen, allowing the user to practice the ideal pace based on visual feedback.

6.4 Grip Controller

The fourth application is the grip of bicycles, which could be employed for driving simulators and actual personal mobilities such as an electric scooter. It can detect twists at the base of the grip and can be used for acceleration control. Figure 19 shows a prototype of the grip-type sensor.

Although electric personal mobility has become more popular in recent years, control interfaces and methods are still uniform. By utilizing this sensor, it is possible to customize the shape, hardness, and input method of the control interface to suit an individual. For example, if a person has a weak grip and has difficulty grasping a lever, but can push or shear, it may be easier to adjust the deformable input, such as applying force backward or with a different body part.

³<https://www.thingiverse.com/thing:693895>



Figure 16: Prototype of a shoe sole with integrated sensors. (a) Force on the sole can be sensed by resistance value. (b) The sensors are placed at the toe and the heel of the sole. (c) Closeup of the sensor part.

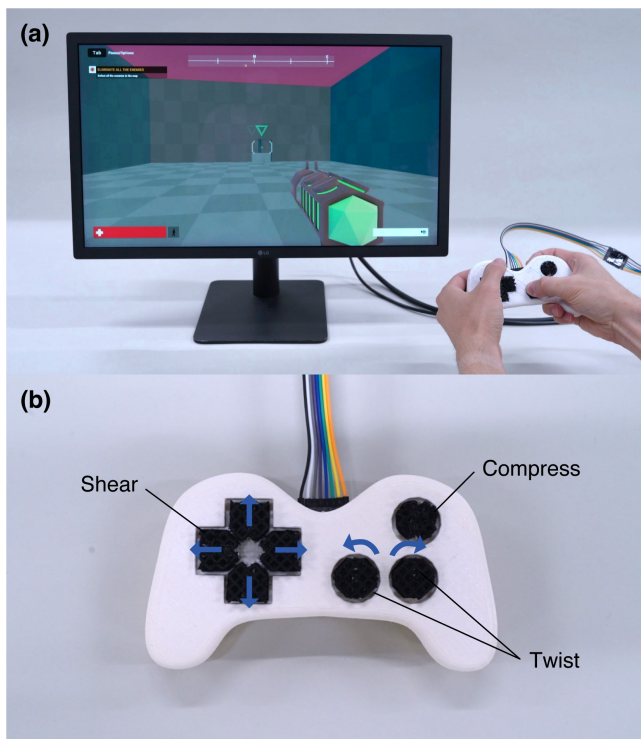


Figure 17: Photo of the game controller prototype. (a) An example of playing a first-person shooter game with the LattiSense controller. (b) Each button provides unique passive haptic feedback according to its function.

LattiSense allows the user to freely select the mode of deformation; therefore, the control method can be optimized to each user.

Research has been conducted on incorporating touch sensors into 3D-printed bike handlebars [Swaminathan et al. 2019]. However, they leverage capacitive touch sensing which is vulnerable to wet environments. Since bike handlebars are mainly used outdoors, exposed to rain and snow, the resistive sensing method has an advantage.

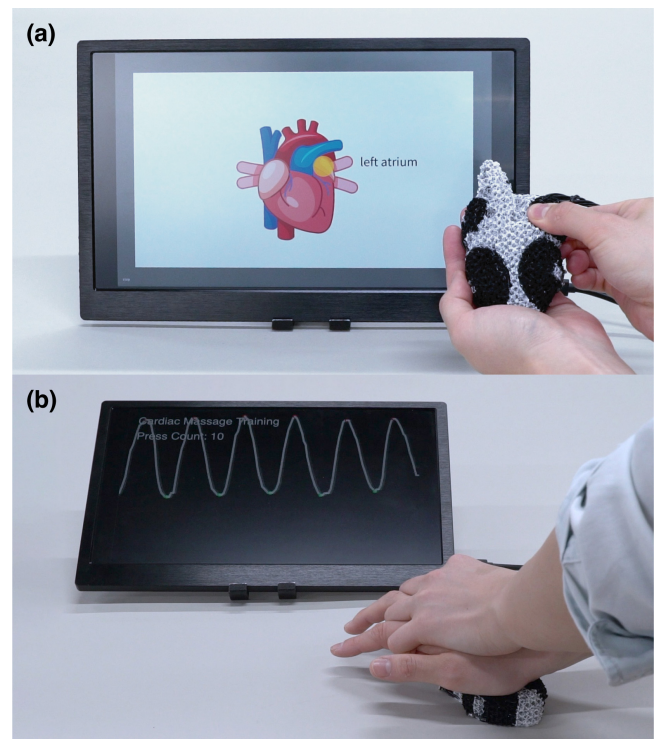


Figure 18: Application example of an educational instrument. (a) Users can memorize the part by checking the shape of the heart in their hands. (b) Cardiac massage training example.

7 LIMITATIONS AND FUTURE WORK

7.1 Durability

In the evaluation section, we evaluated the durability and behavior of the sensor after repeated deformation. However, there is a concern related to anisotropy in FDM technology: The prints show high durability against external forces applied in the printing direction (z-axis) but low durability against the forces applied in the direction perpendicular to the printing direction (x and y axes).

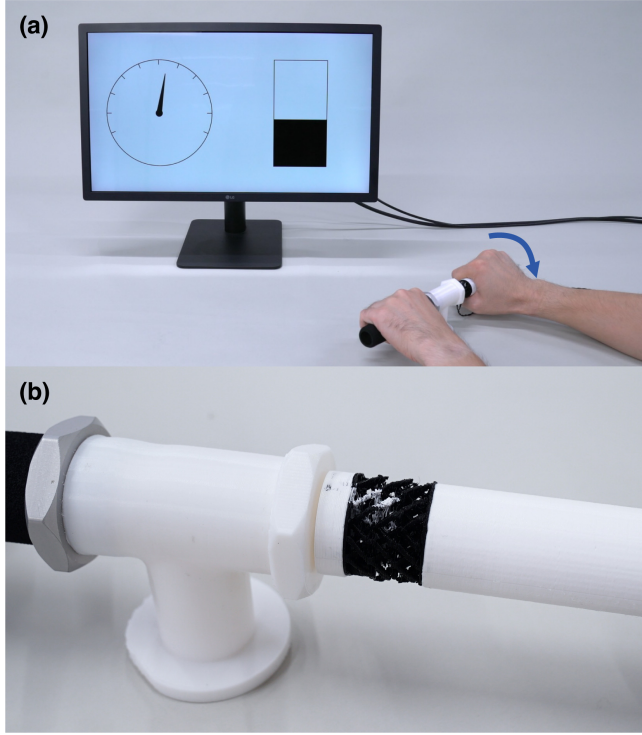


Figure 19: Prototype of the bike grip sensor. (a) When the user twists the grip, the deformation can be detected with an appropriate haptic feedback (rotation). This prototype could be used for driving simulators or future mobility controllers. (b) The entire grip was printed in a single part with a twist deformation structure embedded at the base of the grip.

Therefore, if the deformation direction does not coincide with the build direction, it may not have the aforementioned durability. Our design tool allows embedding soft sensors with various deformation modes in a user's desired deformation direction. Therefore, it is necessary to consider a method that increases the durability of prints for any angles and directions desired by the user.

At present, the fabrication of the sensor is limited to the FDM method. However, the durability of the sensor may be enhanced by the proposed method, which could be extended to other 3D printing technologies, such as Stereolithography (SLA) or Selective Laser Sintering (SLS), due to the improved layer adhesion. Nevertheless, SLA or SLS is currently unsuitable for handling multiple materials and soft conductive materials. Hence, further advancements in these printing technologies are necessary to expand the range of materials that can be utilized for the manufacturing of sensors with improved durability.

Also, when different lattice structures are juxtaposed, there may be durability issues at the connection if there is a large difference in cell size or direction of deformation. A method of smoothly joining the structures should also be considered.

7.2 Wiring and Aggregation

LattiSense consists of conductive and non-conductive flexible filaments that allow wiring points within a single soft sensor to be consolidated into a single place. However, when multiple soft sensors are embedded in a single object, the number of wiring points increases with the number of soft sensors.

The current solution to this problem is to use the internal space of the lattice structure to organize the wiring. For example, in the heart model shown as an application, sensors are embedded in four different parts of the heart. The wires for each sensor are gathered in one place at each area, but furthermore, the wires for these four parts are also gathered in one place by utilizing the space inside the lattice structure. This is an advantage of LattiSense's lattice structure, which has a certain amount of space.

However, with this approach, depending on the number of sensors and the entire shape, the wiring process may be complicated or the internal wires may spoil the softness of the product. Therefore, if the conductive parts could be well designed and utilized as internal wiring to combine the wires of each sensor in one place, the usability of this sensor would be further improved. In this case, the conductive path of one of the sensors may pass through other sensors, and the deformation may affect the resistance of the other sensors, so it is necessary to devise a conductive path that allows the sensors to be distinguished from each other.

Currently, the deformation that can be detected by a single sensor is limited to one deformation type and one direction, and a multimodal sensor is realized by combining several sensors. Therefore, increasing the number of types of deformation that can be detected by a single sensor will also help solve the problem of increased wiring when multiple sensors are combined.

7.3 Design Guideline

The design tool developed in this study allows for the selection of deformation type and sensor softness. However, it is currently difficult to know how the created 3D model will be deformed, how soft it will be, and whether the data is 3D printable until it is printed. However, these soft objects are difficult to simulate in the nonlinear region.

Therefore, we intend to make this sensor more usable by creating design guidelines for users to select the structure and by developing a function in the software to suggest the preferred parameter range based on these guidelines.

For example, in the twist structure, it was difficult to print a structure with a cell size of 6.0 mm and a beam thickness of 0.8 mm, but the combination of these values can be selected on the current software. We will examine the capabilities of more combinations and link each parameter so that the user can select the desired range. Also, there were some experimental results, such as the shear structure having a larger amount of shear when it has a certain hardness and the twist structure having a smaller amount of rotation when the number of cells is increased. We will develop a system to obtain the desired deformation for such deformations.

In addition, the separator is currently a plate shape with a single cell width, but the size and shape of the separator is related to the deformation portion of the object that can be detected. It would

be helpful to investigate the effects of the separator size and shape and to increase the design freedom of the sensing area.

8 CONCLUSION

In this study, we proposed LattiSense, a printable deformable sensor with a three-dimensional shape, fabricated using the FDM technology. This sensor exhibits deformable softness by printing flexible filaments into a lattice structure. We contributed to increasing the degree of freedom in designing three-dimensional shapes, softness, deformation modes, and wiring locations that were difficult to achieve with conventional soft sensors using existing materials by 3D printing conductive flexible filaments in a lattice structure. This enabled the creation of soft and flexible interfaces and products customized for individuals, as shown in the application. We believe that LattiSense can be a new soft sensor to enrich human interaction with soft objects.

ACKNOWLEDGMENTS

This work was supported by Mercari, Inc., Japan and by JSPS KAKENHI Grant Number JP20H05960 and JST, ACT-X Grant Number JPMJAX200M, Japan.

REFERENCES

- Muhammad Abdullah, Romeo Sommerfeld, Laurenz Seidel, Jonas Noack, Ran Zhang, Thijs Roumen, and Patrick Baudisch. 2021. Roadkill: Nesting Laser-Cut Objects for Fast Assembly. In *The 34th Annual ACM Symposium on User Interface Software and Technology* (Virtual Event, USA) (*UIST '21*). Association for Computing Machinery, New York, NY, USA, 972–984. <https://doi.org/10.1145/3472749.3474799>
- Diab W. Abueidda, Mete Bakir, Rashid K. Abu Al-Rub, Jörgen S. Bergström, Nahil A. Sobh, and Iwona Jasiuk. 2017. Mechanical properties of 3D printed polymeric cellular materials with triply periodic minimal surface architectures. *Materials & Design* 122 (2017), 255–267. <https://doi.org/10.1016/j.matdes.2017.03.018>
- Roland Aigner, Mira Alida Haberfellner, and Michael Haller. 2022. SpaceR: Knitting Ready-Made, Tactile, and Highly Responsive Spacer-Fabric Force Sensors for Continuous Input. In *Proceedings of the 35th Annual ACM Symposium on User Interface Software and Technology* (Bend, OR, USA) (*UIST '22*). Association for Computing Machinery, New York, NY, USA, Article 68, 15 pages. <https://doi.org/10.1145/3526113.3545694>
- Marwa Alalawi, Noah Pacik-Nelson, Junyi Zhu, Ben Greenspan, Andrew Doan, Brandon M Wong, Benjamin Owen-Block, Shanti Kaylene Mickens, Wilhelm Jacobus Schoeman, Michael Wessely, Andreea Danilescu, and Stefanie Mueller. 2023. MechSense: A Design and Fabrication Pipeline for Integrating Rotary Encoders into 3D Printed Mechanisms. In *Proceedings of the 2023 CHI Conference on Human Factors in Computing Systems* (Hamburg, Germany) (*CHI '23*). Association for Computing Machinery, New York, NY, USA, Article 626, 14 pages. <https://doi.org/10.1145/3544548.3581361>
- Bernd Bickel, Moritz Bächer, Miguel A. Otraduy, Hyunho Richard Lee, Hanspeter Pfister, Markus Gross, and Wojciech Matusik. 2010. Design and Fabrication of Materials with Desired Deformation Behavior. *ACM Trans. Graph.* 29, 4, Article 63 (jul 2010), 10 pages. <https://doi.org/10.1145/1778765.1778800>
- Alberto Boem and Giovanna Maria Troiano. 2019. Non-Rigid HCI: A Review of Deformable Interfaces and Input. In *Proceedings of the 2019 on Designing Interactive Systems Conference* (San Diego, CA, USA) (*DIS '19*). Association for Computing Machinery, New York, NY, USA, 885–906. <https://doi.org/10.1145/3322276.3322347>
- Zheren Cai, Shengdong Zhao, Zhandong Huang, Zheng Li, Meng Su, Zeying Zhang, Zhipeng Zhao, Xiaotian Hu, Yue-Sheng Wang, and Yanlin Song. 2019. Bubble architectures for locally resonant acoustic metamaterials. *Advanced Functional Materials* 29, 51 (2019), 1906984.
- Corentin Coulais, Eial Teomy, Koen De Reus, Yair Shokef, and Martin Van Hecke. 2016. Combinatorial design of textured mechanical metamaterials. *Nature* 535, 7613 (2016), 529–532.
- Mustafa Doga Dogan, Faraz Faruqi, Andrew Day Churchill, Kenneth Friedman, Leon Cheng, Sriram Subramanian, and Stefanie Mueller. 2020. G-ID: Identifying 3D Prints Using Slicing Parameters. In *Proceedings of the 2020 CHI Conference on Human Factors in Computing Systems* (Honolulu, HI, USA) (*CHI '20*). Association for Computing Machinery, New York, NY, USA, 1–13. <https://doi.org/10.1145/3313831.3376202>
- Nikola A Dudukovic, Erika J Fong, Hawi B Gameda, Joshua R DeOtte, Maira R Cerón, Bryan D Moran, Jonathan T Davis, Sarah E Baker, and Eric B Duoss. 2021. Cellular fluidics. *Nature* 595, 7865 (2021), 58–65. <https://doi.org/10.1038/s41586-021-03603-2>
- Charles El Helou, Philip R Buskohl, Christopher E Tabor, and Ryan L Harne. 2021. Digital logic gates in soft, conductive mechanical metamaterials. *Nature Communications* 12, 1 (2021), 1633. <https://doi.org/10.1038/s41467-021-21920-y>
- Antonia Georgopoulou, Bram Vanderborght, and Frank Clemens. 2021. Multi-material 3D Printing of Thermoplastic Elastomers for Development of Soft Robotic Structures with Integrated Sensor Elements. In *Industrializing Additive Manufacturing*, Mirko Meboldt and Christoph Klahn (Eds.). Springer International Publishing, Cham, 67–81.
- Jun Gong, Olivia Seow, Cedric Honnet, Jack Forman, and Stefanie Mueller. 2021. MetaSense: Integrating Sensing Capabilities into Mechanical Metamaterial. Association for Computing Machinery, New York, NY, USA, 1063–1073. <https://doi.org/10.1145/3472749.3474806>
- Changyo Han, Ryo Takahashi, Yuchi Yahagi, and Takeshi Naemura. 2021. 3D Printing Firm Inflatables with Internal Tethers. In *Extended Abstracts of the 2021 CHI Conference on Human Factors in Computing Systems* (Yokohama, Japan) (*CHI EA '21*). Association for Computing Machinery, New York, NY, USA, Article 218, 7 pages. <https://doi.org/10.1145/3411763.3451613>
- Md. Hazrat Ali, Sagidolla Batai, and Dulat Karim. 2021. Material minimization in 3D printing with novel hybrid cellular structures. *Materials Today: Proceedings* 42 (2021), 1800–1809. <https://doi.org/10.1016/j.matpr.2020.12.185> 3rd International Conference on Materials Engineering & Science.
- Liang He, Gierad Laput, Eric Brockmeyer, and Jon E. Froehlich. 2017. SqueezePulse: Adding Interactive Input to Fabricated Objects Using Corrugated Tubes and Air Pulses. In *Proceedings of the Eleventh International Conference on Tangible, Embedded, and Embodied Interaction* (Yokohama, Japan) (*TEI '17*). Association for Computing Machinery, New York, NY, USA, 341–350. <https://doi.org/10.1145/3024969.3024976>
- Liang He, Huaishu Peng, Michelle Lin, Ravikanth Konjeti, François Guimbretière, and Jon E. Froehlich. 2019. Ondulé: Designing and Controlling 3D Printable Springs. In *Proceedings of the 32nd Annual ACM Symposium on User Interface Software and Technology* (New Orleans, LA, USA) (*UIST '19*). Association for Computing Machinery, New York, NY, USA, 739–750. <https://doi.org/10.1145/3332165.3347951>
- Scott E. Hudson. 2014. Printing Teddy Bears: A Technique for 3D Printing of Soft Interactive Objects. In *Proceedings of the SIGCHI Conference on Human Factors in Computing Systems* (Toronto, Ontario, Canada) (*CHI '14*). Association for Computing Machinery, New York, NY, USA, 459–468. <https://doi.org/10.1145/2556288.2557338>
- Alexandra Ion, Johannes Fröhnhofen, Ludwig Wall, Robert Kovacs, Mirela Alistar, Jack Lindsay, Pedro Lopes, Hsiang-Ting Chen, and Patrick Baudisch. 2016. Metamaterial Mechanisms. In *Proceedings of the 29th Annual Symposium on User Interface Software and Technology* (Tokyo, Japan) (*UIST '16*). Association for Computing Machinery, New York, NY, USA, 529–539. <https://doi.org/10.1145/2984511.2984540>
- Alexandra Ion, Robert Kovacs, Oliver S. Schneider, Pedro Lopes, and Patrick Baudisch. 2018. Metamaterial Textures. In *Proceedings of the 2018 CHI Conference on Human Factors in Computing Systems* (Montreal QC, Canada) (*CHI '18*). Association for Computing Machinery, New York, NY, USA, 1–12. <https://doi.org/10.1145/3173574.3173910>
- Benjamin Jenett, Christopher Cameron, Filippos Tourlomousis, Alfonso Parra Rubio, Megan Ochalek, and Neil Gershenfeld. 2020. Discretely assembled mechanical metamaterials. *Science Advances* 6, 47 (2020), eabc9943. <https://doi.org/10.1126/sciadv.abc9943>
- Yuki Kubo, Kana Eguchi, and Ryosuke Aoki. 2020. 3D-Printed Object Identification Method Using Inner Structure Patterns Configured by Slicer Software. In *Extended Abstracts of the 2020 CHI Conference on Human Factors in Computing Systems* (Honolulu, HI, USA) (*CHI EA '20*). Association for Computing Machinery, New York, NY, USA, 1–7. <https://doi.org/10.1145/3334480.3382847>
- Ajeet Kumar, Saurav Verma, and Jeng-Ywan Jeng. 2020. Supportless lattice structures for energy absorption fabricated by fused deposition modeling. *3D Printing and Additive Manufacturing* 7, 2 (2020), 85–96. <https://doi.org/10.1089/3dp.2019.0089>
- Joanne Leong, Jose Martinez, Florian Perteneder, Ken Nakagaki, and Hiroshi Ishii. 2020. WraPr: Spool-Based Fabrication for Object Creation and Modification. In *Proceedings of the Fourteenth International Conference on Tangible, Embedded, and Embodied Interaction* (Sydney NSW, Australia) (*TEI '20*). Association for Computing Machinery, New York, NY, USA, 581–588. <https://doi.org/10.1145/3374920.3374990>
- Yiyue Luo, Kui Wu, Tomás Palacios, and Wojciech Matusik. 2021. KnitUI: Fabricating Interactive and Sensing Textiles with Machine Knitting. In *Proceedings of the 2021 CHI Conference on Human Factors in Computing Systems* (Yokohama, Japan) (*CHI '21*). Association for Computing Machinery, New York, NY, USA, Article 668, 12 pages. <https://doi.org/10.1145/3411764.3445780>
- Kathryn H Matlack, Anton Bauhofer, Sebastian Krödel, Antonio Palermo, and Chiara Darai. 2016. Composite 3D-printed metastructures for low-frequency and broadband vibration absorption. *Proceedings of the National Academy of Sciences* 113, 30 (2016), 8386–8390.
- Stefanie Mueller, Tobias Mohr, Kerstin Guenther, Johannes Fröhnhofen, and Patrick Baudisch. 2014. FaBrickation: Fast 3D Printing of Functional Objects by Integrating Construction Kit Building Blocks. In *Proceedings of the SIGCHI Conference on Human Factors in Computing Systems* (Toronto, Ontario, Canada) (*CHI '14*). Association for Computing Machinery, New York, NY, USA, 459–468. <https://doi.org/10.1145/2556288.2557338>

- Computing Machinery, New York, NY, USA, 3827–3834. <https://doi.org/10.1145/2556288.2557005>
- Satoshi Nakamaru, Ryosuke Nakayama, Ryuma Niizuma, and Yasuaki Kakehi. 2017. FoamSense: Design of Three Dimensional Soft Sensors with Porous Materials. In *Proceedings of the 30th Annual ACM Symposium on User Interface Software and Technology* (Québec City, QC, Canada) (*UIST '17*). Association for Computing Machinery, New York, NY, USA, 437–447. <https://doi.org/10.1145/3126594.3126666>
- Vinh Nguyen, Pramod Kumar, Sang Ho Yoon, Ansh Verma, and Karthik Ramani. 2015. SOFTii: Soft Tangible Interface for Continuous Control of Virtual Objects with Pressure-Based Input. In *Proceedings of the Ninth International Conference on Tangible, Embedded, and Embodied Interaction* (Stanford, California, USA) (*TEI '15*). Association for Computing Machinery, New York, NY, USA, 539–544. <https://doi.org/10.1145/2677199.2687898>
- Patrick Parzer, Adwait Sharma, Anita Vogl, Jürgen Steinle, Alex Olwal, and Michael Haller. 2017. SmartSleeve: Real-Time Sensing of Surface and Deformation Gestures on Flexible, Interactive Textiles, Using a Hybrid Gesture Detection Pipeline. In *Proceedings of the 30th Annual ACM Symposium on User Interface Software and Technology* (Québec City, QC, Canada) (*UIST '17*). Association for Computing Machinery, New York, NY, USA, 565–577. <https://doi.org/10.1145/3126594.3126652>
- Huaishu Peng, Jennifer Mankoff, Scott E. Hudson, and James McCann. 2015. A Layered Fabric 3D Printer for Soft Interactive Objects. In *Proceedings of the 33rd Annual ACM Conference on Human Factors in Computing Systems* (Seoul, Republic of Korea) (*CHI '15*). Association for Computing Machinery, New York, NY, USA, 1789–1798. <https://doi.org/10.1145/2702123.2702327>
- Jesús Pérez, Bernhard Thomaszewski, Stelian Coros, Bernd Bickel, José A. Canabal, Robert Sumner, and Miguel A. Otaduy. 2015. Design and Fabrication of Flexible Rod Meshes. *ACM Trans. Graph.* 34, 4, Article 138 (jul 2015), 12 pages. <https://doi.org/10.1145/2766998>
- Rei Sakura, Changyo Han, Keisuke Watanabe, Ryosuke Yamamura, and Yasuaki Kakehi. 2022. Design of 3D-Printed Soft Sensors for Wire Management and Customized Softness. In *Extended Abstracts of the 2022 CHI Conference on Human Factors in Computing Systems* (New Orleans, LA, USA) (*CHI EA '22*). Association for Computing Machinery, New York, NY, USA, Article 192, 5 pages. <https://doi.org/10.1145/3491101.3519906>
- Martin Schmitz, Jürgen Steinle, Jochen Huber, Niloofar Dezfuli, and Max Mühlhäuser. 2017. Flexibles: Deformation-Aware 3D-Printed Tangibles for Capacitive Touchscreens. In *Proceedings of the 2017 CHI Conference on Human Factors in Computing Systems* (Denver, Colorado, USA) (*CHI '17*). Association for Computing Machinery, New York, NY, USA, 1001–1014. <https://doi.org/10.1145/3025453.3025663>
- Christian Schumacher, Bernd Bickel, Jan Rys, Steve Marschner, Chiara Daraio, and Markus Gross. 2015. Microstructures to Control Elasticity in 3D Printing. *ACM Trans. Graph.* 34, 4, Article 136 (jul 2015), 13 pages. <https://doi.org/10.1145/2766926>
- Julia Schwarz, Chris Harrison, Scott Hudson, and Jennifer Mankoff. 2010. Cord Input: An Intuitive, High-Accuracy, Multi-Degree-of-Freedom Input Method for Mobile Devices. In *Proceedings of the SIGCHI Conference on Human Factors in Computing Systems* (Atlanta, Georgia, USA) (*CHI '10*). Association for Computing Machinery, New York, NY, USA, 1657–1660. <https://doi.org/10.1145/1753326.1753573>
- Fereshteh Shahmiri, Chaoyang Chen, Anandghan Waghmare, Dingtian Zhang, Shivan Mittal, Steven L. Zhang, Yi-Cheng Wang, Zhong Lin Wang, Thad E. Starner, and Gregory D. Abowd. 2019. Serpentine: A Self-Powered Reversibly Deformable Cord Sensor for Human Input. In *Proceedings of the 2019 CHI Conference on Human Factors in Computing Systems* (Glasgow, Scotland UK) (*CHI '19*). Association for Computing Machinery, New York, NY, USA, 1–14. <https://doi.org/10.1145/3290605.3300775>
- Ronit Slyper, Ivan Poupyrev, and Jessica Hodgins. 2010. Sensing through Structure: Designing Soft Silicone Sensors. In *Proceedings of the Fifth International Conference on Tangible, Embedded, and Embodied Interaction* (Funchal, Portugal) (*TEI '11*). Association for Computing Machinery, New York, NY, USA, 213–220. <https://doi.org/10.1145/1935701.1935744>
- Lingyun Sun, Yu Chen, Deying Pan, Yue Yang, Yitao Fan, Jiaji Li, Ziqian Shao, Ye Tao, and Guanyun Wang. 2021a. FlexCube: 3D Printing Tunable Meta-Structures with Triply Periodic Minimal Surfaces. In *Extended Abstracts of the 2021 CHI Conference on Human Factors in Computing Systems*. Association for Computing Machinery, New York, NY, USA, Article 190, 4 pages. <https://doi.org/10.1145/3411763.3451562>
- Lingyun Sun, Jiaji Li, Yu Chen, Yue Yang, Zhi Yu, Danli Luo, Jianzhe Gu, Lining Yao, Ye Tao, and Guanyun Wang. 2021b. FlexTruss: A Computational Threading Method for Multi-Material, Multi-Form and Multi-Use Prototyping. In *Proceedings of the 2021 CHI Conference on Human Factors in Computing Systems* (Yokohama, Japan) (*CHI '21*). Association for Computing Machinery, New York, NY, USA, Article 432, 12 pages. <https://doi.org/10.1145/3411764.3445311>
- Lingyun Sun, Yue Yang, Yu Chen, Jiaji Li, Danli Luo, Haolin Liu, Lining Yao, Ye Tao, and Guanyun Wang. 2021c. ShrinCage: 4D Printing Accessories That Self-Adapt. In *Proceedings of the 2021 CHI Conference on Human Factors in Computing Systems* (Yokohama, Japan) (*CHI '21*). Association for Computing Machinery, New York, NY, USA, Article 433, 12 pages. <https://doi.org/10.1145/3411764.3445220>
- Saiganesh Swaminathan, Kadri Bugra Oztemiz, Carmel Majidi, and Scott E. Hudson. 2019. FiberWire: Embedding Electronic Function into 3D Printed Mechanically Strong, Lightweight Carbon Fiber Composite Objects. In *Proceedings of the 2019 CHI Conference on Human Factors in Computing Systems* (Glasgow, Scotland UK) (*CHI '19*). Association for Computing Machinery, New York, NY, USA, 1–11. <https://doi.org/10.1145/3290605.3300797>
- Ryan L. Truby, Lillian Chin, Annan Zhang, and Daniela Rus. 2022. Fluiddic innervation sensorizes structures from a single build material. *Science Advances* 8, 32 (2022), eabq4385. <https://doi.org/10.1126/sciadv.abq4385> arXiv:<https://www.science.org/doi/10.1126/sciadv.abq4385>
- Liang Wang and Hai-Tao Liu. 2020. 3D compression-torsion cubic mechanical metamaterial with double inclined rods. *Extreme Mechanics Letters* 37 (2020), 100706. <https://doi.org/10.1016/j.eml.2020.100706>
- Keisuke Watanabe, Ryosuke Yamamura, and Yasuaki Kakehi. 2021. foamin: A Deformable Sensor for Multimodal Inputs Based on Conductive Foam with a Single Wire. In *Extended Abstracts of the 2021 CHI Conference on Human Factors in Computing Systems*. Association for Computing Machinery, New York, NY, USA, Article 189, 4 pages. <https://doi.org/10.1145/3411763.3451547>
- Tony Wu, Shihui Fukuhara, Nicholas Gillian, Kishore Sundara-Rajan, and Ivan Poupyrev. 2020. ZebraSense: A Double-Sided Textile Touch Sensor for Smart Clothing. In *Proceedings of the 33rd Annual ACM Symposium on User Interface Software and Technology* (Virtual Event, USA) (*UIST '20*). Association for Computing Machinery, New York, NY, USA, 662–674. <https://doi.org/10.1145/3379337.3415886>
- Wenjun Wu, Pai Liu, and Zhan Kang. 2021. A novel mechanical metamaterial with simultaneous stretching- and compression-expanding property. *Materials & Design* 208 (2021), 109930. <https://doi.org/10.1016/j.matdes.2021.109930>
- Kenta Yamamoto, Ryota Kawamura, Kazuki Takazawa, Hiroyuki Osone, and Yoichi Ochiai. 2021. A Preliminary Study for Identification of Additive Manufactured Objects with Transmitted Images. In *Artificial Intelligence in HCI: Second International Conference, AI-HCI 2021, Held as Part of the 23rd HCI International Conference, HCII 2021, Virtual Event, July 24–29, 2021, Proceedings*. Springer-Verlag, Berlin, Heidelberg, 439–458. https://doi.org/10.1007/978-3-030-77772-2_29
- Willa Yungi Yang, Yunmeng Zhuang, Luke Andre Darcy, Grace Liu, and Alexandra Ion. 2022. Reconfigurable Elastic Metamaterials. In *Proceedings of the 35th Annual ACM Symposium on User Interface Software and Technology* (Bend, OR, USA) (*UIST '22*). Association for Computing Machinery, New York, NY, USA, Article 67, 13 pages. <https://doi.org/10.1145/3526113.3545649>
- Sang Ho Yoon, Ke Huo, Yunbo Zhang, Guiming Chen, Luis Paredes, Subramanian Chidambaram, and Karthik Ramani. 2017. Isof: A Customizable Soft Sensor with Real-Time Continuous Contact and Stretching Sensing. In *Proceedings of the 30th Annual ACM Symposium on User Interface Software and Technology* (Québec City, QC, Canada) (*UIST '17*). Association for Computing Machinery, New York, NY, USA, 665–678. <https://doi.org/10.1145/3126594.3126654>
- Sang Ho Yoon, Luis Paredes, Ke Huo, and Karthik Ramani. 2018. MultiSoft: Soft Sensor Enabling Real-Time Multimodal Sensing with Contact Localization and Deformation Classification. *Proc. ACM Interact. Mob. Wearable Ubiquitous Technol.* 2, 3, Article 145 (sep 2018), 21 pages. <https://doi.org/10.1145/3264955>
- Yaoyao Fiona Zhao Yunlong Tang. 2016. A survey of the design methods for additive manufacturing to improve functional performance. *Rapid Prototyping Journal* 22, 3 (2016), 569–590. <https://doi.org/10.1108/RPJ-01-2015-0011>
- Jiani Zeng, Honghao Deng, Yunyi Zhu, Michael Wessely, Axel Kilian, and Stefanie Mueller. 2021. Lenticular Objects: 3D Printed Objects with Lenticular Lens Surfaces That Can Change Their Appearance Depending on the Viewpoint. In *The 34th Annual ACM Symposium on User Interface Software and Technology* (Virtual Event, USA) (*UIST '21*). Association for Computing Machinery, New York, NY, USA, 1184–1196. <https://doi.org/10.1145/3472749.3474815>
- Xiuhai Zhang, Zhiguo Qu, and Hui Wang. 2020. Engineering acoustic metamaterials for sound absorption: from uniform to gradient structures. *Iscience* 23, 5 (2020), 101110.
- Rongchang Zhong, Minghui Fu, Xuan Chen, Binbin Zheng, and Lingling Hu. 2019. A novel three-dimensional mechanical metamaterial with compression-torsion properties. *Composite Structures* 226 (2019), 111232. <https://doi.org/10.1016/j.compstruct.2019.111232>